

“Innovative high pressure/high temperature, multi-sensing bioreactors system for microbial risk assessment in underground hydrogen storage”

Original

“Innovative high pressure/high temperature, multi-sensing bioreactors system for microbial risk assessment in underground hydrogen storage” / Vasile, Nicolò Santi; Bellini, Ruggero; Bassani, Ilaria; Vizzarro, Arianna; Abdel Azim, Annalisa; Coti, Christian; Barbieri, Donatella; Scapolo, Matteo; Viberti, Dario; Verga, Francesca; Pirri, Fabrizio; Menin, Barbara. - In: INTERNATIONAL JOURNAL OF HYDROGEN ENERGY. - ISSN 0360-3199. - 51:(2024), pp. 41-50. [10.1016/j.ijhydene.2023.10.245]

Availability:

This version is available at: 11583/2983952 since: 2023-11-20T08:27:35Z

Publisher:

International Journal of Hydrogen Energy

Published

DOI:10.1016/j.ijhydene.2023.10.245

Terms of use:

This article is made available under terms and conditions as specified in the corresponding bibliographic description in the repository

Publisher copyright

(Article begins on next page)

Lossy transmission line response via numerical Laplace Transform inversion

I. Maio
Dip. Elettronica
Politecnico
Torino, Italy
(+39) 11-564-4100
maio@polito.it

F. G. Canavero
Dip. Elettronica
Politecnico
Torino, Italy
(+39) 11-564-4060
canavero@polito.it

ABSTRACT

An efficient transient analysis of lossy lines with nonlinear loads requires the ability to compute and represent a suitable set of line impulse responses. In this paper, we propose the evaluation of the matched-line impulse responses by means of an algorithm for the numerical inversion of the Laplace Transform. Based on a discussion of the structure of the impulse responses, we demonstrate how, for this class of functions, the method proposed is particularly effective and convenient, in comparison with the conventional FFT approach. We also compare the line responses due to the exact per-unit-length resistance of a circular wire with those due to a simplified model, and find a non negligible influence on the integrity of the signals that propagate on the line.

INTRODUCTION

Owing to the diffusion of nonlinear devices and the tendency towards decreasing rise times of the signal waveforms, the transient analysis of multiconductor transmission lines has become of central importance in the study of complex electric and electronic systems. In the last years, a great deal of work has been done on this subject and now many interesting solution scheme are available. In particular, the approach consisting in characterizing the line with impulse responses and solving transient equations at the line ends looks very promising (e.g., see papers in [1, 2]). An example of this technique is given by the two matched transient scattering equations

$$b_1(t) = s_{21}(t) * a_2(t), \quad b_2(t) = s_{21}(t) * a_1(t), \quad (1)$$

characterizing the lossy line, and the two reflection equations for the terminal loads ($p = 1, 2$)

$$-y_0(t) * (a_p(t) - b_p(t)) = g_p(a_p(t) + b_p(t) - e_p(t)), \quad (2)$$

where y_0 is the line transient characteristic admittance, g_p represents the possibly nonlinear load characteristic and e_p is a source term. Besides, though this set of equations describes a scalar line, its matrix extension to the case of a lossy multiconductor line is straightforward, by means of the modal decomposition [3].

To be feasible and convenient, however, the approach based the line transient characterization requires the ability to compute and represent a suitable set of line impulse responses. Such requirement is not trivial to be met, because the line responses affect the precision and the efficiency of the transient simulation. In this paper, we propose the evaluation of the line impulse responses of (1) and (2) by means of an algorithm for the numerical inversion of the Laplace Transform [4]. We choose the impulse responses arising from the matched scattering formulation, since it seems that this line representation is best suited for the inverse transformation.

Last, please note that, throughout the paper, lower case letters denote time domain variables and upper case letters indicate their counterparts in the frequency domain.

RLC LINE CHARACTERISTICS

In the case of the matched scattering characterization, a lossy line, whose per-unit-length parameters are L , C , and $R(s)$ (G is neglected, since its effects usually take place only at very high frequencies), is described in terms of a transmission function

$$S_{21} = H(s) = e^{-\gamma(s)\mathcal{L}}, \quad \gamma(s) = \frac{s}{v} \sqrt{1 + \frac{R(s)}{sL}}, \quad (3)$$

and a characteristic admittance

$$Y_0(s) = Y_{LC} / \sqrt{1 + \frac{R(s)}{sL}}. \quad (4)$$

where s is the complex angular frequency, \mathcal{L} is the line

length, $v = 1/\sqrt{LC}$ is its phase speed, and $Y_{LC} = \sqrt{C/L}$ is the LC -characteristic admittance.

The line characteristics are expressed here in the frequency domain, as it is natural. However, for the time domain approach of (1) and (2), the transmission impulse response of the matched line $h(t)$, and the transient characteristic admittance $y_0(t)$, are needed.

MATCHED-LINE RESPONSE

In order to obtain a better insight into the structure of the line impulse response, it is convenient to introduce the following normalized time and complex frequency quantities:

$$T = \nu t, \quad S = \Sigma + j\Omega = s/\nu, \quad (5)$$

where $\nu = vR(0)Y_{LC}$. Also, the numerical evaluation of $h(t)$ is facilitated by the extraction of the asymptotic linear phase $s\mathcal{L}/v$ (that causes a time delay $\tau = \mathcal{L}/v$ in $h(t)$) from the propagation factor γ . Then we concentrate on the inverse transformation of

$$\bar{H}(S) = e^{-G(S)}, \quad G(S) = S\xi \left\{ \sqrt{1 + \frac{r(S)}{S}} - 1 \right\}, \quad (6)$$

where $\xi = Y_{LC}R(0)\mathcal{L}$, $r(S) = R(S\nu)/R(0)$, and we obtain $h(t) = \nu\bar{h}(\nu(t - \tau))$. It should be pointed out that the normalized line delay $T = \nu\tau = \nu\mathcal{L}/v$ coincides with ξ .

In order to deal with an explicit form of (6), we consider the simple per-unit-length resistance model of a coaxial cable [5], i.e.,

$$r(S) = j\sqrt{S}QJ_0(j2Q\sqrt{S})/J_1(j2Q\sqrt{S}), \quad (7)$$

where J_0 and J_1 are Bessel functions, and $Q = \sqrt{10^{-7}vY_{LC}}$.

Figure 1 shows the numerical approximation of \bar{h} computed from (6) by means of the Hosono algorithm [4], for $Q = 0.547$ (e.g., $v = 3 \times 10^8$ m/s, $Y_{LC} = 0.01 \Omega^{-1}$), and $\xi = 0.1$, $\xi = 5$. Logarithmic scales are needed to visualize on the same plot both the short and the long time parts of the \bar{h} function, since they have markedly different time constants. In order to verify the results of the numerical inversion, it is convenient to take advantage of the fact that the high- and low-frequency approximations of $G(S)$ produce two asymptotically exact short- and long-time parts of \bar{h} [3], i.e.,

$$G_s(S) = \frac{1}{2}\xi Q\sqrt{S} \rightarrow \bar{h}_s(T) = \eta \frac{1}{\sqrt{\pi(T\eta)^3}} \exp\{-1/T\eta\}, \quad (8)$$

$$G_r(S) = S\xi \left\{ \sqrt{1 + \frac{1}{S}} - 1 \right\} \rightarrow \bar{h}_r(T) = \exp\{-\xi/2\} \frac{1}{2} \delta(T/2) + \exp\{-\xi/2\} \frac{\xi}{4} \frac{\exp\{-T/2\}}{\sqrt{T/2(T/2 + \xi)}} I_1(\sqrt{T/2(T/2 + \xi)}), \quad (9)$$

where $\eta = (4/\xi Q)^2$ and I_1 is the modified Bessel function. The shapes of \bar{h}_s and \bar{h}_r are also shown in Fig. 1, on a log-log scale; an example of their appearance on linear scales can be found in [3].

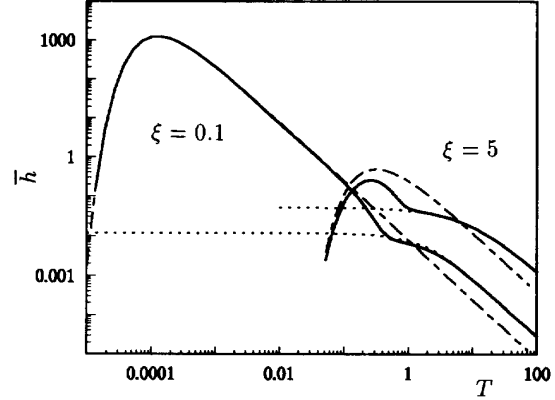


Figure 1: Impulse response $\bar{h}(T)$ of an RLC line, computed by numerical inversion of the Laplace Transform (solid line), and its exact asymptotic behaviors \bar{h}_s and \bar{h}_r (dashed and dotted curves, respectively) ($Q = 0.547$ and $\xi = 0.1, 5$). Logarithmic scales are used for both normalized function and normalized time axes.

The curves of Fig. 1 are useful to assess the dependence of the function \bar{h} on the amount of line losses. For small ξ , \bar{h} nearly coincides with \bar{h}_s for small time values, while, at larger times, \bar{h} nearly coincides with \bar{h}_r . For large ξ , however, \bar{h}_s is inadequate to approximate \bar{h} for small values of T . The transitions between these two behaviours can be estimated around $\xi = 2$. Therefore, the type of the time response can be effectively classified with the help of the parameter ξ . In fact, the impulse response of a line with $\xi < 2$ (*low-loss line*) is characterized by an initial peak due to high-frequency losses, with a duration much shorter than the line delay τ , and a slow evolution for longer times, for which $\bar{h} \propto 1/\sqrt{T^3}$. Additionally, the time instant T_s ($T_s \approx 1$ in Fig. 1) at which \bar{h} of a low-loss line switches from the \bar{h}_s to the \bar{h}_r behaviour appears almost independent of ξ . This means that the impulse response of a low-loss line is mainly determined by skin losses up to $t_s = \nu T_s$, and by DC losses beyond t_s .

The normalized form of (4) is

$$\bar{Y}(S) = Y_0(S\nu)/Y_{LC} = 1/\sqrt{1 + \frac{r(S)}{S}}, \quad (10)$$

and $y_0(t) = \nu\bar{y}(\nu t)$. Figure 2 shows, on a log-log scale, the numerical approximation of $-\bar{y}$ computed from (10) by means of the method [4], and for $Q = 0.547$.

As for \bar{h} , we compare the result of the numerically computed \bar{y} with its exact short- and long-time parts, which

are obtained from the indicated high- and low-frequency approximations of \bar{Y} :

$$\bar{Y}_s(S) = 1 - \frac{Q}{2\sqrt{S}} \rightarrow \bar{y}_s(T) = \delta(T) - \frac{Q}{2\sqrt{\pi T}}, \quad (11)$$

$$\bar{Y}_r(S) = \sqrt{S} \rightarrow \bar{y}_r(T) = -\frac{1}{2\sqrt{\pi T^3}}. \quad (12)$$

The functions $-\bar{y}_s$ and $-\bar{y}_r$ are shown for comparison in Fig. 2.

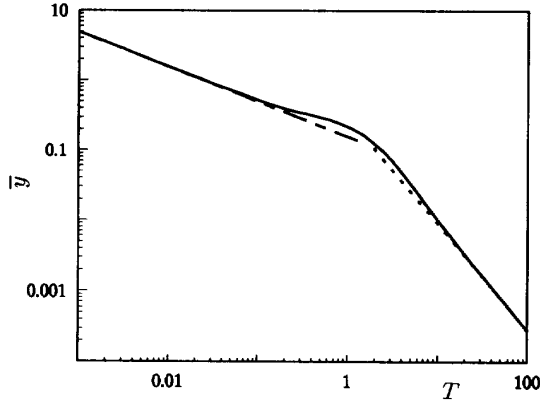


Figure 2: Transient admittance $\bar{y}(T)$ of an RLC line, computed by numerical inversion of the Laplace Transform (solid line), and its exact analytical short- (dashed curve) and long-time (dotted curve) behaviours ($Q = 0.547$). Logarithmic scales are used for both normalized function and normalized time axes.

COMPUTATIONAL COST AND ACCURACY

The difficulty to obtain the line transient impulse responses via the inverse FFT algorithm is widely recognized in the literature. For example, the standard FFT algorithm would require 10^5 uniformly spaced time samples to represent the curves of Fig. 1 for $\xi = 0.1$ in a time window $[0, 10]$ and with a resolution of 10^{-4} . On the contrary, the adoption of a Laplace Transform inversion algorithm, working for arbitrary time points, allows us to effectively evaluate those functions that contain different time scales. In fact, the \bar{h} curves of Fig. 1 were obtained for 50 samples, logarithmically spaced in time, each of which was computed by means of the method [4] that required the function evaluation at 13 frequency values.

The method adopted was tested for the functions G_s and G_r , whose corresponding exact impulse responses are known. Possible values of the method parameters were determined: $k = 10$, $m = 3$, $a = 5$ (the meaning of such parameters is omitted here for brevity: see [4]) and were found adequate to obtain a relative error less than

5×10^{-2} for $T > T_{peak}$, T_{peak} being the time where \bar{h} is maximum.

The closeness of the numerical approximation to both the short- and long-time asymptotic solutions can be directly appreciated from Fig. 1: this is a remarkable feature of the method for this class of functions. Besides, the inherent error of this method for the \bar{h} functions is bounded by $\bar{h}(T) \exp\{-2a\}$ for any $T > T_{peak}$ [4]. However, the approximation error grows for $T \rightarrow 0$, and increasingly higher values of the method parameters (k , m , a) are required to obtain acceptable results at time values smaller than those shown in Fig. 1. Usually, this problem appears only at the very beginning of the approximated curve, where the behaviour of \bar{h} is not relevant (in fact, the line model applies only for a finite band, and therefore the time response is uncertain before a minimum time value); in any case, the inversion method of [6] works effectively for short times, and can be applied, if needed, to reconstruct the initial part of \bar{h} .

Also the transient characteristic admittance is not easily computed via the FFT algorithm. In fact, y_0 has a finite asymptotic value and a singularity of the type $1/\sqrt{t}$ for $t = 0$ (see (4) and Fig. 2), which prevents from a direct application of the FFT inversion.

The accuracy and efficiency considerations given for \bar{h} hold also for \bar{y} , including the agreement with the short- and long-time reference solution. A further remarkable feature is the insensitivity of the numerical method to the $\delta(T)$ term of the impulse response, since the curve of Fig. 2 is obtained without the extraction of the asymptotic part of (10).

EFFECT OF THE RESISTANCE MODEL

An important question, not yet addressed, is the influence of the per-unit-length line resistance model on the line impulse response and on the transient simulations. Regardless of the line transverse geometry, the frequency behaviour of its per-unit-length resistance is usually approximated by the Holt's model [7], whose normalized form reads

$$r_h(S) = 1 + Q'\sqrt{S}, \quad (13)$$

where $Q' \equiv Q$ for a circular wire. Figure 3 compares the \bar{h} functions obtained with the method of [4] for the exact resistance model of a circular wire (7) and for the Holt's resistance model. The impulse responses shown in Fig. 3 mainly differ in the transition between the short- and the long-time regime, where \bar{h} corresponding to the accurate resistance model presents a more pronounced kink. This is explained by the observation that the time interval where the impulse responses differ corresponds to the frequency interval where the resistance models switch from the DC to the skin effect behaviour: in this

region, the approximated resistance model is smoother than the accurate one.

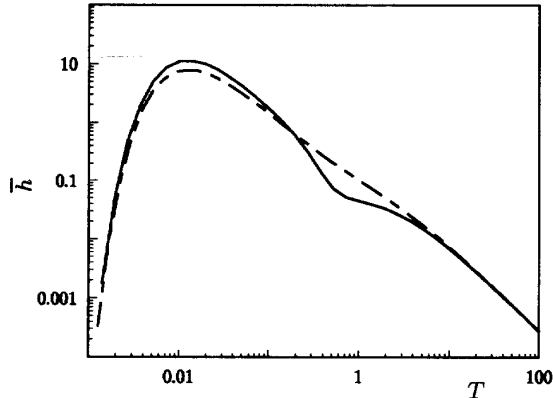


Figure 3: Comparison of \bar{h} functions of a coaxial RLC line obtained with the approximate resistance model (dashed curve) and with the exact resistance model (solid curve). ($Q = 0.547$, $\xi = 1$).

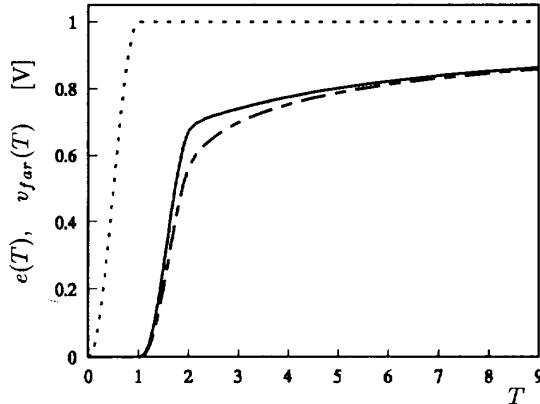


Figure 4: Far-end response of a matched line computed by means of the impulse responses of Fig. 3. The solid line refers to the exact resistance model, the dashed line to the approximate model, and the dotted line is the input signal.

This difference can have a non negligible influence on the deformation of the signals that propagate on the line, and this consideration provides a good motivation for the application of the proposed numerical inversion methods that are able to handle more accurate line parameter models. We believe that this motivation applies also to the work of [8], where, however, no discussion of the impulse response structure and of the results obtained is given.

As an example, Fig. 4 shows the voltage signal at the end of a matched transmission line for the two impulse responses of Fig. 3 and for a raised cosine input signal of amplitude 1 V and unit normalized rise time. The dif-

ferent waveform distortion estimated by the two models can be clearly seen.

CONCLUSIONS

Impulse responses of RLC lines are analysed with the help of a numerical Laplace Transform inversion algorithm. This approach is shown to be well suited in this case, since two very different time scales are present in the function behaviour. In fact, the absence of need for a linear sampling increases the efficiency of this method over the conventional FFT algorithm. Additionally, this method guarantees a very good accuracy of the results at a reduced computational cost and is superior to the FFT algorithm. Finally, we can handle more accurate models of the frequency dependence of the per-unit-length line parameters. The results of this work can be exploited for an efficient and accurate implementation of the transient analysis of electrical networks containing nonlinear elements interconnected by lossy and possibly multiconductor lines.

REFERENCES

- [1] W. W. M. Dai, Special Issue on *Simulation, modeling and electrical design of high-speed and high-density interconnects*, *IEEE Trans. Circuits Syst.-I*, 39, 11, November 1992.
- [2] M. Nakhla and Q. J. Zhang, Special Issue on *High-speed interconnects*, *Int. J. Analog Integrated Circuits and Signal Processing*, 5, 1, January 1994.
- [3] I. Maio, S. Pignari e F. G. Canavero, "Efficient transient analysis of nonlinearly loaded low-loss interconnects," *Int. J. Analog Integrated Circuits and Signal Processing*, 5, 1, pp.7-17 January 1994.
- [4] T. Hosono, "Numerical inversion of Laplace transform and some applications to wave optics," *Radio Science*, 16, pp.1015-1019, November 1981.
- [5] R. E. Matick, *Transmission Lines for Digital and Communications Networks*, New York: McGraw-Hill, 1969.
- [6] J. R. Griffith and M. Nakhla, "Time-domain analysis of lossy coupled transmission lines," *IEEE Trans. Microwave Theory Tech.*, MTT-38, pp.1480-1487, October 1990.
- [7] D. R. Holt, "Expansions with coefficient algorithms for time domain responses of skin effect lossy coaxial cables," *J. Res. Nat. Bur. Stand.*, B (Math. Sci.), 74B, 3, pp.155-173, July-Sept. 1970.
- [8] E. C. Chang and S. Kang, "Computationally efficient simulation of a lossy transmission line with skin effect by using numerical inversion of Laplace Transform," *IEEE Trans. Circuits Syst.-I*, 39, pp.861-868, November 1992.